

FIG. 1. The two lowest-energy states of B<sub>3</sub> possess singly occupied orbitals of  $\sigma_{a_1'}$  (a) and  $\pi_{a_1'}$  (b) symmetries, respectively.

tween the monovalent H and Li atoms. Our findings are detailed below in Sec. III.

## II. CHOICE OF ATOMIC ORBITAL BASIS SETS AND ELECTRONIC CONFIGURATIONS

For boron, the study was carried out using the  $[9s4p1d/3s2p1d]$  correlation-consistent basis atomic orbital basis set of Dunning,<sup>3</sup> chosen because it is capable of treating electron correlation. No corresponding basis set for lithium has, to our knowledge, been developed. Thus the 6-311 G\* basis of Krishnan, Binkley, Seeger, and Pople<sup>4</sup> was chosen for lithium because of its ability to reproduce bond lengths and bond energies.<sup>5</sup> The polarization function on Li is due to Binkley and Pople.<sup>6</sup>

Because of the ionic nature of B<sub>3</sub>Li, use of additional diffuse *s* and *p* basis functions from Clark *et al.*<sup>7</sup> was considered, because, in some regions of the potential energy surfaces of B<sub>3</sub>Li, the charge density has B<sub>3</sub><sup>-</sup>Li<sup>+</sup> character. However, inclusion of these diffuse functions increased the predicted electron affinity of B<sub>3</sub> by only 5 kcal/mol. Hence, the remainder of this study was carried out without these extra diffuse functions to expedite the calculation, and (small) corrections for resultant errors in state energies that correlate to B<sub>3</sub><sup>-</sup> were made.

Our choice of electronic configurations is designed to provide a qualitatively correct treatment of low-lying states, but not to achieve a high-level treatment of dynamical electron correlation. We employed the complete active space multiconfiguration self-consistent field (CAS-MCSCF) method to this end. For C<sub>3v</sub> geometries, which produced some of the more interesting results reported here, the two lowest-energy totally symmetric (*a*<sub>1</sub>) orbitals and the lowest energy degenerate pair of *e*-type molecular

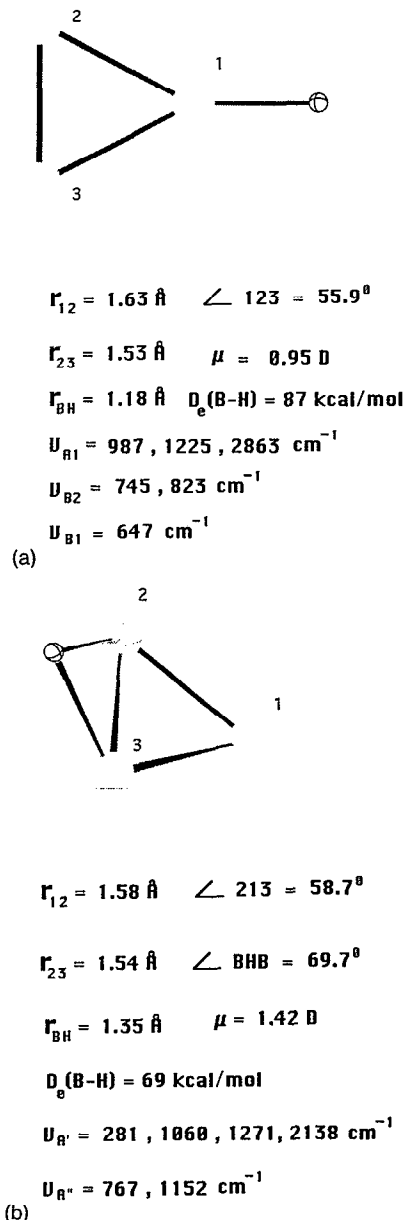


FIG. 2. Two stable structures of B<sub>3</sub>H, the  $\sigma$ -bonded structure (a) and the bridge-bonded structure (b).

orbitals were doubly occupied in all configuration state functions (CSFs). These four frozen core orbitals correspond to the three B 1*s* and the Li 1*s* orbitals. The remaining ten electrons were distributed in all possible ways among the next four *a*<sub>1</sub> orbitals and the next two degenerate pairs of *e* orbitals. Qualitatively, these eight orbitals describe the three B–B  $\sigma$  bonds (*a*<sub>1</sub> and *e*), the three B-atom nonbonding orbitals (*a*<sub>1</sub> and *e*) and the bonding and antibonding four-center B<sub>3</sub>–Li orbitals (both of *a*<sub>1</sub> symmetry). This choice of active orbital space resulted in 1176 CSFs of singlet spin multiplicity.

Before deciding on the above choice for the active orbital space, we examined alternatives. In particular, the roles of the three B–B  $\sigma^*$  orbitals (*a*<sub>1</sub> and *e*) and the two B<sub>3</sub>  $\pi^*$  orbitals (*e*) that do not couple to the Li 2*s* orbital needed to be addressed. Because we had knowledge from

earlier work of our group on the electron affinity (EA) of  $B_3$  and because such energy differences involving different electron numbers pose special difficulties, we decided to compute this EA for various active orbital choices. The primary result of these studies is that the computed EA of  $B_3$  varied by no more than 0.3 eV when the active orbital space (for both  $B_3$  and  $B_3^-$ ) was increased by the orbitals mentioned above. The EA was found to be largest when the size of the active orbital space was largest. Because we were concerned that truncation of the active orbital space would overestimate the EA, the latter observation was reassuring. The result of numerous such tests lead us to the eight-active-orbital ten-electron valence space introduced above; this choice allowed us to handle, in a computationally feasible manner, the many geometrical "walks" on the ground state surface (which required analytical first and second energy derivatives) needed to locate the stable geometries reported here.

### III. SUMMARY OF FINDINGS

#### A. $B_3Li$ Stable structures

Although we found a stable  $C_{2v}$   $\sigma$ -bonded  $B_3Li$  structure analogous to the  $B_3H$  structure shown in Fig. 2(a), the analog of the bridge-bonded structure of Fig. 2(b) was found to be not stable. The Li-B bond energy for the stable  $C_{2v}$   $\sigma$ -bonded species is  $D_e=47$  kcal/mol, and it has a dipole moment of  $\mu=8.50$  D. Its geometry and local harmonic vibrational frequencies are described in Fig. 3(a).

A  $C_{3v}$  four-center structure is also predicted to be geometrically stable, and, in fact, to be the global minimum for this species (the analog  $C_{3v}$  structure of  $B_3H$  was found to be geometrically unstable with respect to displacement of the Li atom in the plane of the  $B_3$  moiety). This  $B_3Li$  structure lies 13 kcal/mol below the above  $\sigma$ -bonded species and has a dissociation energy to produce ( $X^2A_1$ )  $B_3 + Li$  of  $D_e=60$  kcal/mol. Its geometry and local harmonic vibrational frequencies are described in Fig. 3(b). The dipole moment of this molecule is  $\mu=6.7$  D, which corresponds to a fractional charge transfer of  $q=0.64 e^-$  from Li to the center of the  $B_3$  plane. The relatively large electron affinity of  $B_3$  ( $\sim 1.5$  eV as computed in this work, compared to 0.28 eV for the B atom) is the source of this high degree of charge transfer.

#### B. Charge-transfer nature of the $B_3Li$ bonding

The  $B_3Li$  molecule provides an interesting study in bonding and structure because of the presence of several low-energy electronic states. For  $C_{3v}$  geometries, as the Li atom is withdrawn from the center of the  $B_3$  triangle, the dipole moment  $\mu$  increases as shown in Fig. 4 where the lowest energy singlet state is labeled  $^1A_1$ . From the dipole moment it is clear that the electronic nature of the  $X^1A$   $B_3Li$  state changes drastically near  $R \cong 4.2-5.2$  Å, where the molecule evolves from a charge-transfer complex in which  $q \cong 0.6$  to one in which one valence electron resides on the Li atom and one remains with the  $B_3$  moiety. Over this range of  $R$  values, the dipole moment  $\mu$  decreases from 12 to 1.5 D.

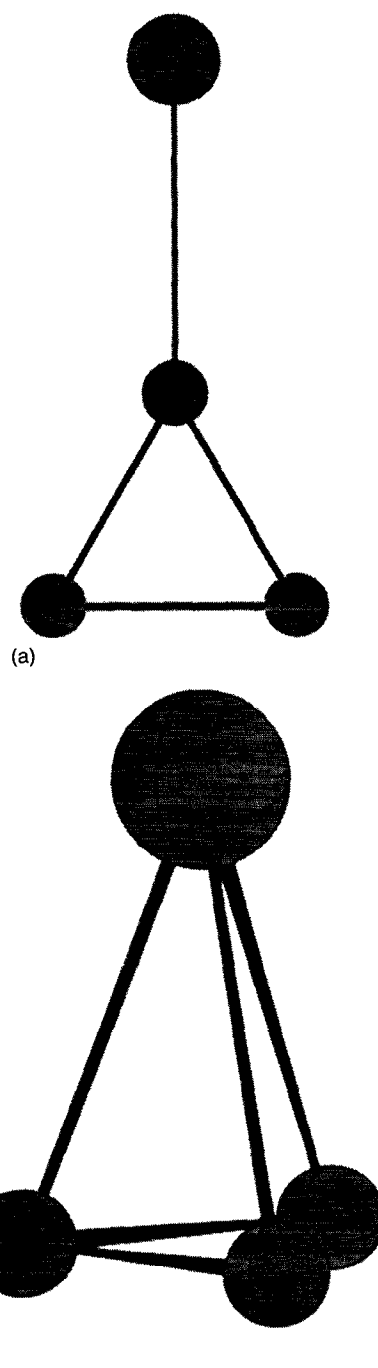


FIG. 3. (a) The  $C_{2v}$   $\sigma$ -bonded structure of  $B_3Li$ . The vibrational frequencies (in  $cm^{-1}$ ) and their symmetries are: 76( $b_1$ ), 78( $b_2$ ), 433( $a_1$ ), 923( $a_1$ ), 971( $b_2$ ), 1254( $a_1$ ). The B-Li bond length is 2.15 Å, the two equal B-B bond lengths are 1.58 Å, and the unique B-B bond length is 1.56 Å. (b) The  $C_{3v}$  lowest-energy structure of  $B_3Li$ . The vibrational frequencies (in  $cm^{-1}$ ) and their symmetries are: 237( $e$ ), 452( $a_1$ ), 954( $e$ ), 1251( $a_1$ ). The B-B bond lengths are 1.57 Å, and the B-Li distance is 2.18 Å.

Dissociation of the  $C_{3v}$  structure of  $B_3Li$  discussed above produces  $B_3$  in its  $X^2A'_1$  state and Li ( $^2S$ ). Dissociation of the  $C_{2v}$   $\sigma$ -bonded  $B_3Li$  structure also produces  $B_3$  in its ground state and Li ( $^2S$ ), so both structures lie on the same potential energy surface. The large dipole moment (8.5 D) of the  $\sigma$ -bonded structure indicates that charge transfer also plays an important role in its bonding.

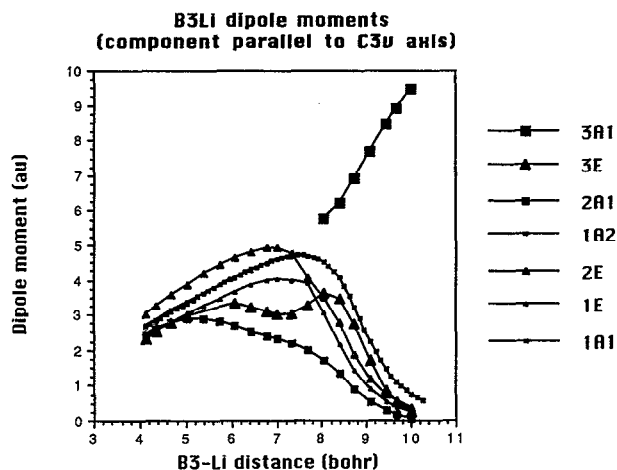


FIG. 4. Dipole moments (1 a.u. = 2.54 D) of several low-lying singlet electronic states of  $C_{3v}$   $B_3Li$  as a function of the  $B_3$ -Li distance (in bohr = 0.529 Å units). The state labeled  $3A_1$  (the third state of  $A_1$  symmetry) dissociates to  $B_3^- + Li^+$ ; the other states all correlate to  $B_3 + Li$  asymptotically. The states of  $E$  symmetry cause the lowest vibrational frequency of  $e$  symmetry to be quite small, but do not render the in-plane movement of the Li atom geometrically unstable (see the text).

### C. Stability of the $C_{3v}$ structure of $B_3Li$ and instability of $C_{3v}$ $B_3H$

The appearance of low-energy excited states of  $^1E$  symmetry had a profound role in determining the instability of the  $C_{3v}$  structure in  $B_3H$  and the stability of the corresponding  $C_{3v}$  structure of  $B_3Li$ . Second order Jahn-Teller coupling of the  $X^1A_1$  and low-energy  $^1E$  states of  $B_3H$ , induced by distortions of  $e$  symmetry (e.g., movement of the H atom parallel to the  $B_3$  plane) caused the  $^1A_1$  surface to be geometrically unstable at such  $C_{3v}$  geometries. In the present  $B_3Li$  case, low-lying  $^1E$  states are again present; the lowest state lies  $\sim 80$  kcal/mol above the  $^1A_1$  ground state at the  $C_{3v}$  geometry of Fig. 3(b). However, unlike the  $B_3H$  analog, the second order Jahn-Teller couplings between the  $^1E$  and  $^1A_1$  states are not strong enough to render the  $^1A_1$  state unstable with respect to  $e$ -symmetry motion of the

Li center. As a result, the  $C_{3v}$  geometry is stable for  $B_3Li$ , even though it was unstable for  $B_3H$ .

## IV. SUMMARY

The primary findings reported here are

(1)  $B_3Li$  has been found to possess two geometrically stable isomers—one of  $C_{3v}$  symmetry and a second  $\sigma$ -bonded structure of  $C_{2v}$  symmetry. The two isomers differ in electronic energy by 13 kcal/mol. Both involve charge transfer in their ground state bonding, and thus have very large dipole moments (6.7 and 8.5 D, respectively).

(2) Both isomers dissociate to ground state  $B_3$  (which has an electron affinity of  $\sim 1.5$  eV) and Li ( $^2S$ ); the former with  $D_e = 60$  kcal/mol, the latter with  $D_e = 47$  kcal/mol.

(3) No stable bridge-bonded structure analogous to that of  $B_3H$  was found to be stable for  $B_3Li$ .

(4) The presence of low-lying excited states of  $^1E$  symmetry does not render the  $C_{3v}$  structure of  $B_3Li$  second order Jahn-Teller unstable; for  $B_3H$ , the corresponding  $^1E$  states do cause the  $C_{3v}$  structure to be geometrically unstable.

(5) The large electronegativity difference between H and Li makes the bonding and structures that arise in  $B_3Li$  quite different from those in  $B_3H$ .

## ACKNOWLEDGMENTS

This work was supported in part by the Office of Naval Research and by NSF Grants No. CHE8814765 and CHE9116286. We also thank the Utah Supercomputer Institute for staff and computer resources.

<sup>1</sup>R. Hernandez and J. Simons, *J. Chem. Phys.* **94**, 2961 (1991).

<sup>2</sup>R. Hernandez and J. Simons, *J. Chem. Phys.* **96**, 8251 (1992).

<sup>3</sup>T. Dunning, *J. Chem. Phys.* **90**, 1007 (1989).

<sup>4</sup>R. Krishnan, J. S. Binkley, R. Seeger, and J. A. Pople, *J. Chem. Phys.* **72**, 650 (1980).

<sup>5</sup>A. B. Sannigrahi, T. Kar, B. G. Niyogi, P. Hobza, and P. v. R. Schleyer, *Chem. Rev.* **90**, 1061 (1990).

<sup>6</sup>J. S. Binkley and J. A. Pople, *J. Chem. Phys.* **66**, 879 (1977).

<sup>7</sup>T. Clark, J. Chandrasekhar, G. W. Spitznagel, and P. v. R. Schleyer, *J. Comp. Chem.* **4**, 294 (1983).